

## Modeling the Ion Selectivity of the Phosphate Specific Channel OprP

Niraj Modi,<sup>†</sup> Roland Benz,<sup>†</sup> Robert E. W. Hancock,<sup>‡</sup> and Ulrich Kleinekathöfer\*,<sup>†</sup>

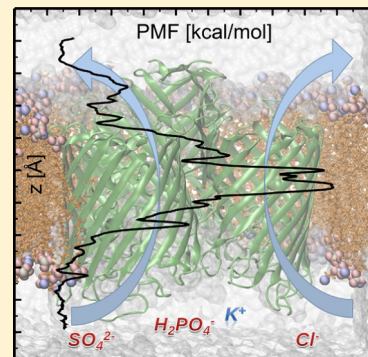
<sup>†</sup>School of Engineering and Science, Jacobs University Bremen, Campus Ring 1, 28759 Bremen, Germany and

<sup>‡</sup>Centre for Microbial Diseases and Immunity Research, Department of Microbiology and Immunology, University of British Columbia, Vancouver, Canada

### Supporting Information

**ABSTRACT:** Ion selectivity of transport systems is an essential property of membranes from living organisms. These entities are used to regulate multifarious biological processes by virtue of selective participation of specific ions in transport processes. To understand this process, we studied the phosphate selectivity of the OprP porin from *Pseudomonas aeruginosa* using all-atom free-energy molecular dynamics simulations. These calculations were performed to define the energetics of phosphate, sulfate, chloride, and potassium ion transport through OprP. Atomic-level analysis revealed that the overall electrostatic environment of the channel was responsible for the anion selectivity of the channel, whereas the particular balance of interactions between the permeating ions and water as well as channel residues drove the selectivity between different anions. The selectivity of OprP is discussed in light of well-studied ion channels that are highly selective for potassium or chloride.

### SECTION: Biophysical Chemistry and Biomolecules



Many biological processes involve the participation of specific ions. The differentiation between ions and ion types is critically important for the functions of biological units. For example, potassium channels selectively and rapidly facilitate the movement of  $K^+$  ions out of the cell and at the same time prevent the entry of  $Na^+$  ions, thus maintaining the necessary electrochemical gradient across the cell membrane, which is essential for the survival of the cell.<sup>1</sup> Likewise, ions contribute significantly toward the structure and function of many proteins and enzymes. Binding of the wrong ion type can disrupt the activity of such molecules.<sup>2</sup> High selectivity is achieved by specific membrane proteins that collectively regulate the appropriate ionic concentration gradients across the different compartments of biological systems and the majority of them belong to the family of ion channels.<sup>1</sup> The ability to discriminate between different ions with a high efficiency is fundamental to their functions. Understanding the structure–function relationship of such ion channels is therefore critical due to their biological importance, for example, as drug targets to treat diseases<sup>3</sup> and to design ion-selective man-made nanopores for various applications, such as water desalination.<sup>4</sup> It is believed that such ion selectivity is the result of a fine-tuned balance of a variety of interactions between ions, proteins, water molecules, and the membrane environment. Although quantifying such interactions is not trivial, molecular dynamics (MD) free-energy simulations provide important tools to identify and quantify microscopic factors responsible for selectivity and complement experimental studies.

Several ion-selective channels and membrane proteins like the KcsA channel,<sup>5–11</sup> the ClC channel,<sup>12</sup> the NaK channel,<sup>7,13</sup>

the nicotinic acetylcholine receptor (nAChR),<sup>14</sup> and others have been investigated using MD simulations and free-energy calculations. In addition, nonselective porins like OmpF were also probed to understand the energetics of various antibiotics transport and modulation of binding sites in the presence of other ions.<sup>15,16</sup> Among the ion-selective channels, the potassium channel KcsA has been thoroughly studied to address the issue of selectivity and in many cases serves as a benchmark system as to how to probe selectivity in other channels. Among the different mechanisms suggested for the selectivity of this channel, the first one was the “snug-fit hypothesis”, which attributed the selectivity to the slight difference in atomic sizes of  $Na^+$  and  $K^+$ .<sup>17</sup> This hypothesis was subsequently ruled out when considering the atomic fluctuations in the binding site, which are larger than the differences in ionic radii.<sup>11</sup> The alternative “field-strength hypothesis” attributes the selectivity to the number and/or physical properties of the ligands coordinating the permeating ions,<sup>10,11</sup> whereas the “over-coordination hypothesis” assigns the selectivity to the number of coordinating ligands only and not their physical properties.<sup>5,6</sup>

Among the various membrane proteins, the outer membrane of Gram negative bacteria contains a special class of proteins called porins.<sup>18</sup> These porins have a  $\beta$ -barrel architecture, and most of them are relatively nonspecific general diffusion channels (e.g., OmpF and OmpC of enteric bacteria). Exceptions are the porins that selectively transport carbohy-

Received: October 11, 2012

Accepted: November 21, 2012

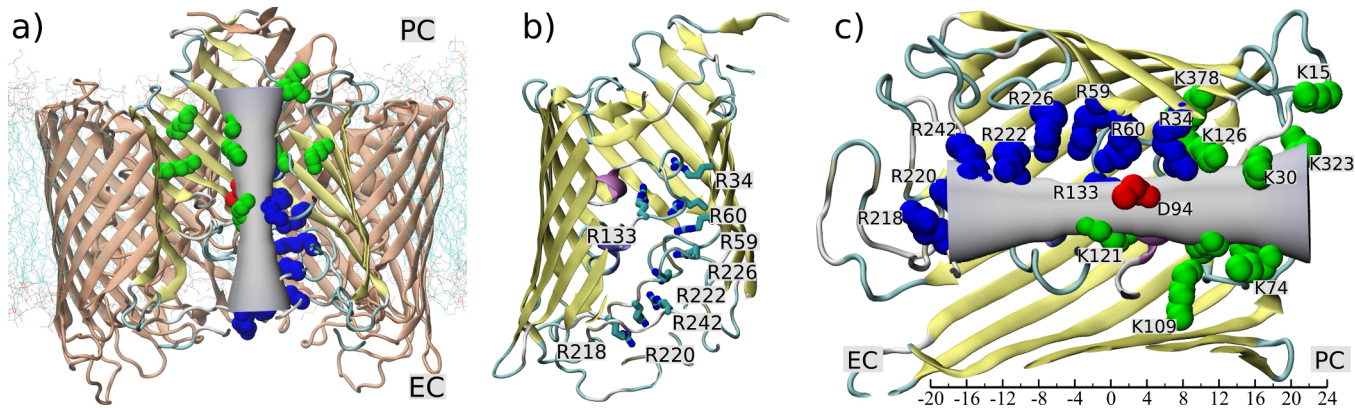


**Figure 1.** OprP structural features. (a) OprP trimer embedded in lipid membrane. The pore of one of the monomers is shown with a gray hourglass shape to indicate the approximate relative radius of the pore in different regions and to guide the eye to the possible pathway for ion permeation. Important charged residues are shown as spheres (Arg-blue, Lys-green, Asp-red). (b) Residues of the Arginine-ladder shown as sticks. (c) Important charged residues are labeled and mapped to their position along the  $z$  axis.

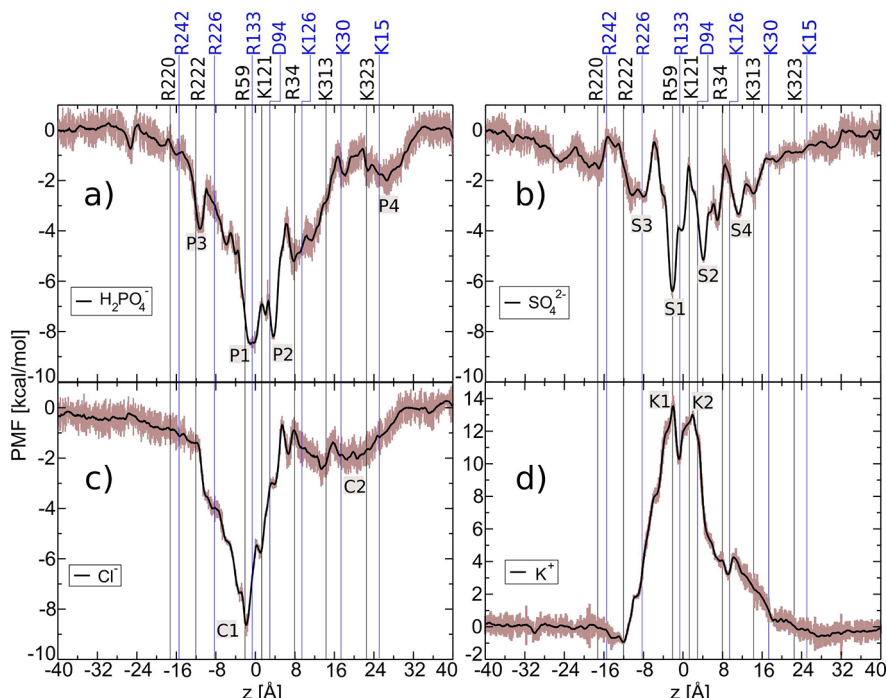


**Figure 2.** PMF profiles for the permeation of (a)  $\text{H}_2\text{PO}_4^-$ , (b)  $\text{SO}_4^{2-}$ , (c)  $\text{Cl}^-$ , and (d)  $\text{K}^+$  ions through OprP. Important residues of OprP along the ion permeation pathway are mapped onto the PMF profiles with respect to their positions along the  $z$  axis. The PMF curve has been averaged over five data points, and important binding site regions/barriers are also labeled. The error bars are shown in brown.

dicates (ScrY and LamB), nucleosides (Tsx), and phosphate ions (OprP). In particular, the high phosphate-selectivity of OprP represents an interesting ion selectivity property that is not common to the porin class of proteins. OprP is an integral outer membrane protein of *Pseudomonas aeruginosa* and is involved in high-affinity uptake of phosphate under phosphate starvation conditions.<sup>19</sup> Under such circumstances, phosphate permeation is  $\sim 20$  times higher than the  $\text{Cl}^-$  transport, as indicated by electrophysiological experiments.<sup>20–22</sup> This is largely due to the 100–500 times higher binding affinity of OprP for phosphate compared with chloride.<sup>20–22</sup>

The crystal structure of OprP revealed its trimeric architecture in which each monomer is formed by 16  $\beta$  strands having extracellular and periplasmic loops (Figure 1).<sup>23</sup> Loops L3, L5, and T7 (Figure S1 of the Supporting Information) play an important role in channel formation. Some of the important

structural features that drive the anion-selectivity of the channel are the so-called arginine ladder including R218, R220, R242, R222, R226, R59, R60, and R34 that extends from the extracellular side down the channel to the middle of the pore, the central phosphate binding site (D94, Y62, S124, S125, K121, K126, R34, R133), and a lysine cluster (K13, K15, K25, K30, K74, K109, K313, K323, K378) on the periplasmic side of the channel (Figure 1). Positively charged Arg and Lys residues are also present in nonspecific porins like OmpF, where they help to facilitate the transport of negatively charged antibiotics with carboxylic groups.<sup>15</sup>

An initial MD simulation study with OprP suggested permeation mechanisms for phosphate and chloride ions.<sup>24</sup> The selectivity of phosphate over chloride was attributed to the differential hydration properties of these two ions on the periplasmic side of the channel due to their different sizes.

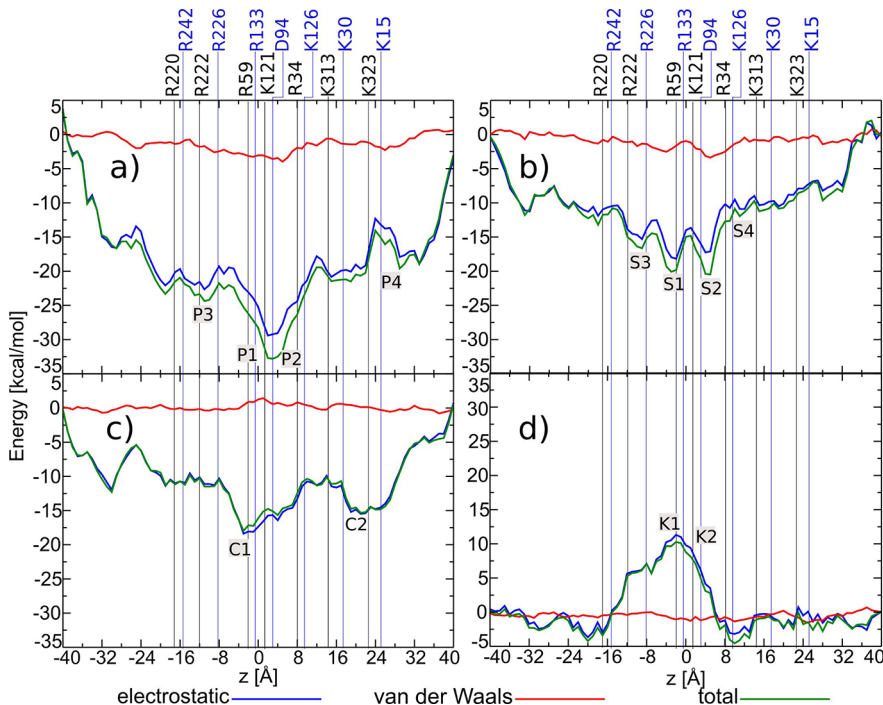


**Figure 3.** Electrostatic and van der Waals interaction energy components for the permeation of (a)  $\text{H}_2\text{PO}_4^-$ , (b)  $\text{SO}_4^{2-}$ , (c)  $\text{Cl}^-$ , and (d)  $\text{K}^+$  ions through OprP. Important residues of OprP along the ion permeation pathway are mapped with respect to their position along the  $z$  axis. Regions of binding sites/barriers are also labeled as per identified in PMF profiles. All energy values denote relative interaction energies assuming zero interaction energies in the bulk.

Apart from unequal sizes of the permeating ions, there seems to be other factors that may also contribute significantly toward the high phosphate selectivity of the pore. For example, OprP also has  $\sim 20$  times higher affinity for phosphate binding than for sulfate, even though phosphate and sulfate ions are similar in size.<sup>20</sup> Hence differential selectivity within anions (binding affinities are in the order of phosphate, sulfate, and chloride, from high to low), as obtained by electrophysiological measurements of OprP,<sup>20</sup> needs to be further analyzed on the atomic scale. Furthermore, it is interesting to investigate factors responsible for the selectivity of this relatively wide porin channel compared with well-studied and relatively narrow, inflexible ion channels. Because of flexible side chains, OprP can be called a “brush-like” nanopore. To achieve detailed understanding of the selectivity in OprP, we employed full atomistic free-energy MD simulations to obtain the energetics of phosphate, chloride, and sulfate ion transport through OprP. As an extreme case, we also studied the energetics of cation transport with potassium as example. Applied-field simulations as for previously performed for  $\alpha$ -hemolysin,<sup>25</sup> MscS,<sup>26</sup> OmpF,<sup>27,28</sup> and OmpC<sup>29</sup> and reviewed in ref 30, were not preferred for OprP due to the small ion currents within a limited simulation time.

Details of the system setup and MD simulations are given in the Supporting Information. In our study, we have considered the monovalent form of phosphate ( $\text{H}_2\text{PO}_4^-$ , different from the one in ref 24) and divalent sulfate ( $\text{SO}_4^{2-}$ ) anion, as they are the most common protonation states around the physiological pH of 7. To determine the effective free-energy profiles for the transport of different ions through OprP, the adaptive biasing force (ABF)<sup>31,32</sup> method, as implemented in the *collective variable* module of NAMD 2.8 program,<sup>33</sup> was utilized. The principal axis of the channel was aligned parallel to the  $z$  axis,

and the reaction coordinate was defined as the  $z$  position of the ion.

The individual 1D potential of mean force (PMF) for the transport of each of four ions,  $\text{H}_2\text{PO}_4^-$ ,  $\text{SO}_4^{2-}$ ,  $\text{Cl}^-$ , and  $\text{K}^+$ , through OprP is shown in Figure 2. All four ions had characteristically different PMF profiles with the generalization that the three anions have energetically favorable binding regions while the cation has a high permeation barrier. Some of the important residues were mapped onto the PMF profiles based on their approximate positions along the  $z$  axis. The PMF for the phosphate ion revealed two central binding sites, P1 and P2, and two additional minor binding sites, P3 and P4 (Figure 2a). The central binding sites, P1 and P2, were energetically very favorable with well depth of  $\sim 9$  kcal/mol. These two sites were spatially  $\sim 5$  Å apart along the  $z$  axis and with an energy barrier of  $\sim 2$  kcal/mol between them. The presence of the two central binding sites was in agreement with the crystal structure data<sup>23</sup> and the previous simulation study.<sup>24</sup> It is important to note here that the values of the free energy changes observed in our simulations were different from those ref 24. This may be due to the different protonation state of the phosphate ion,  $\text{H}_2\text{PO}_4^-$ , that we used in our study (compared with  $\text{PO}_4^{3-}$ , which is unlikely to be found at physiological pH); the use of different force fields<sup>34</sup> and simulation protocols; or the cooperative effect of ions (in ref 24, three ions, one in each channel, are treated simultaneously). One also needs to keep in mind that PMF calculations for membrane proteins are also reported to be sensitive to simulation details like finite system size and use of nonpolarizable force fields, especially for lipid hydrocarbons of the membrane.<sup>34</sup> Nevertheless, the form of the PMF profile was rather similar. Binding site P1 corresponded to the residues R59, R60, K121, and R133, whereas site P2 was formed by residues R34, R60, D94, S125, and R133. (Also see Figure S2 in the Supporting Information.) Furthermore, the

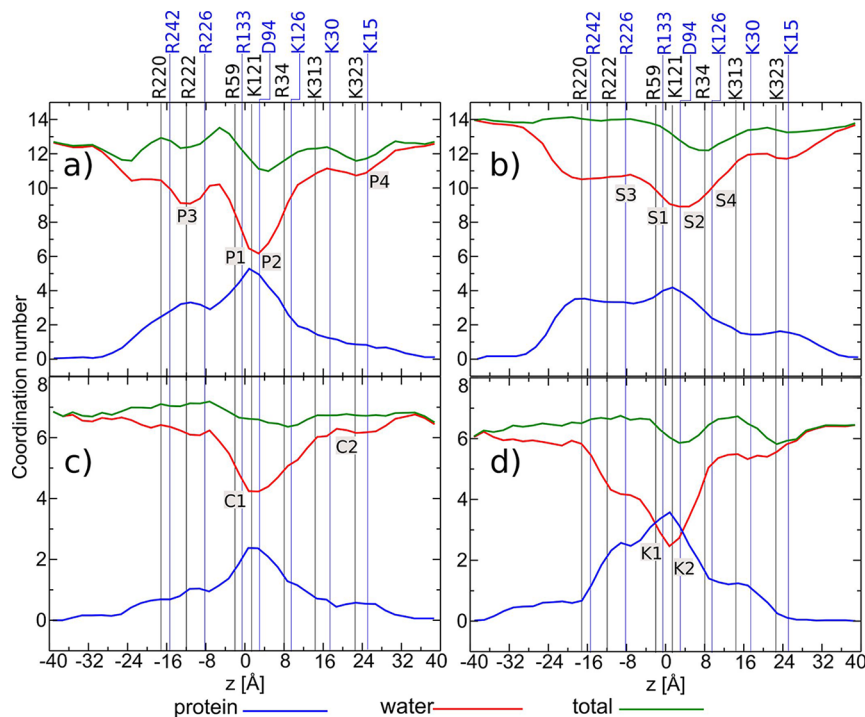


**Figure 4.** Coordination numbers (protein and water contacts) for the permeation of (a)  $\text{H}_2\text{PO}_4^-$ , (b)  $\text{SO}_4^{2-}$ , (c)  $\text{Cl}^-$ , and (d)  $\text{K}^+$  ions through OprP. The regions of binding sites/barriers are also labeled as per definition in the PMF profiles.

minor binding site, P3, on the extracellular side was composed of residues from the arginine ladder, namely, R222, R226, and R242 (Figure S2 in the Supporting Information), and had a well-depth of  $\sim 2$  kcal/mol. Multiple ions can also be included near site P3 due to the large size of the pore in this region. Site P3 along with the other residues of the arginine ladder may act as an entrance funnel to OprP, which increases the local concentration of anions while electrostatically repeling the cations. Another minor binding site, P4, was located on the periplasmic side with contributions from residues of the lysine cluster, K15 and K323. It is worth noting that the overall PMF profile with the existence of prominent central binding sites is different from that of ion channels such as KcsA, where the free-energy landscapes are quite flat with minor local binding sites along the permeation pathway.

The free-energy landscape for sulfate ion transport again showed two central binding sites, S1 and S2 (corresponds to site P1 and P2 for phosphate), and additional local stabilization regions, S3 (corresponding to P3 for phosphate) and S4 (Figure 2b). The depth of the central binding region is  $\sim 7$  kcal/mol with an energy barrier of  $\sim 4$  kcal/mol between binding sites S1 and S2. In contrast, the PMF for the small monatomic  $\text{Cl}^-$  ion showed only one central binding site (corresponds to site P1 for phosphate) with an energy well depth similar to that of phosphate (Figure 2c). Similar positions of the energy wells for phosphate and chloride ions were also reported in ref 24. Additional minor local stabilization regions could be observed around the residues of the lysine cluster (site C2). The different PMF profiles for the anions, especially the variations in the magnitude of the energetic stabilization in the binding regions and the overall pore attractive volume, were consistent with the selectivity between anions as observed in electrophysiological experiments.<sup>20</sup> As expected, the free-energy profile for the  $\text{K}^+$  ion had huge energetic barriers (K1 and K2, corresponds to P1 and P2 for phosphate) of 13 kcal/mol,

making the channel practically impermeable for this ion type (Figure 2d). No significant local stabilization regions are found for  $\text{K}^+$  along the entire length of the pore. The calculated dissociation constants ( $K_d$ ) based on PMF profiles (see the Supporting Information for details) are found to be  $0.23 \mu\text{M}$ ,  $0.72 \mu\text{M}$ ,  $23.3 \mu\text{M}$ , and  $14.9 \text{ mM}$  for  $\text{H}_2\text{PO}_4^-$ ,  $\text{Cl}^-$ ,  $\text{SO}_4^{2-}$ , and  $\text{K}^+$ , respectively.

To investigate further the contributions of individual interaction components toward the selectivity of OprP, namely, electrostatic and van der Waals, the interaction energies were calculated for each permeating ion in the different regions of the pore (Figure 3). For this purpose, the pore was divided into bins of  $1 \text{ \AA}$  in size, and the energies were averaged in each bin. Such an analysis revealed that the electrostatic component of the energy was the major contributor toward determining the overall transport properties of ions through OprP, with very minor contributions from van der Waals interactions. The phosphate ion experienced very favorable electrostatic interaction energies compared with the bulk, indicating an overall positive electrostatic potential inside the pore formed by the presence of the positively charged arginine and lysine residues. The binding sites/barrier regions deduced from the PMF profiles are denoted in Figure 3 for the sake of comparison. The phosphate ion had a strong electrostatic interaction with the central binding site regions, P1 and P2, and also more favorable local interaction energies in minor binding sites (Figure 3a). This indicates the role of the electrostatic energy component in the formation of binding sites.

Similarly the two other anions, sulfate and chloride, experienced favorable electrostatic interactions inside the pore with stronger interactions in the binding site regions (Figure 3b,c). Although the magnitudes of the electrostatic interaction energies were different for each anion, these difference could not be interpreted directly in terms of selectivity as it is necessary to take into account a loss of configurational entropy

upon the binding of ions inside the pore which would lead to a penalty in the overall binding affinity.<sup>35</sup> These types of entropic penalties are the results of motional restrictions of the ions in the confined environment inside the channel and in particular in binding sites. (See Figure S5 of the Supporting Information.) The larger ions,  $\text{H}_2\text{PO}_4^-$  and  $\text{SO}_4^{2-}$ , tended to have higher entropic penalties compared with small ions like  $\text{Cl}^-$ . In contrast with the anions,  $\text{K}^+$  ions had unfavorable electrostatic energies, particularly in the central region of the pore where the diameter was quite narrow (Figure 3d). On the basis of these findings, it could be concluded that the overall electrostatic environment of the OprP channel conferred its anion selectivity.

A more detailed analysis of the interactions between permeating ions, water, channel and their interplay is required to understand further the selectivity between different anions. For example, in the case of the KcsA channel, the selectivity for  $\text{K}^+$  was suggested to be predominantly affected by the type of the ligands coordinating with the permeating ions (carbonyl oxygen of the channel versus water oxygen), in agreement with the so-called “field-strength hypothesis”.<sup>10</sup> The main idea behind this hypothesis is that different types of coordinating ligands have varying intrinsic physical and electrostatic properties. Hence a change in their relative contribution may confer selectivity to a particular ion. We examined the coordination properties of the permeating ions through OprP. The first hydration shell for each of the four ions was determined based on their radial distribution functions in the bulk region (see Supporting Information for further details, Figure S4). Figure 4 shows the coordination number profiles for each of the permeating ions along the length of the pore and extended toward bulk regions on both sides of the pore. The binding sites/barriers identified in the PMF profiles were also labeled here for the sake of comparison. The oxygen atoms of the water molecules versus the nitrogen atoms of the channel walls were considered as coordinating ligands for the three anions, whereas in the case of  $\text{K}^+$ , oxygen atoms of the channel were considered instead of nitrogen atoms.

The average number of coordinating water molecules decreased as the permeating ions moved from the bulk phase to the channel interior, which was compensated by a higher number of protein contacts with the channel (Figure 4). The total number of coordinating ligands (water versus protein) remained almost constant throughout the channel with minor fluctuations. It is also worth noting that there are pronounced similarities in the changes in water coordination and the corresponding PMFs shown in Figure 2. As a general trend, ions tended to remove more water molecules from the hydration shell in the binding site/barrier regions, which is compensated by a high number of protein contacts. For example, in the case of  $\text{H}_2\text{PO}_4^-$ , the largest number of water molecules was removed in the central binding site regions (P1 and P2), leading to a maximum protein contacts in this regions. Even changes in the number of water molecules were reflected in similar changes in the PMF profiles, as seen for P3 and P4.

In the context of suggested hypotheses of ion selectivity, the “over-coordination hypothesis” justified the selectivity for  $\text{H}_2\text{PO}_4^-$  (coordination number: 13) and  $\text{SO}_4^{2-}$  (coordination number: 14) over  $\text{Cl}^-$  (coordination number: 7) but could not explain the selectivity of  $\text{H}_2\text{PO}_4^-$  over  $\text{SO}_4^{2-}$ . In terms of the “field-strength hypothesis”, the relative contribution from the type of coordinating ligands (water oxygen versus protein nitrogen) was different for both ions types, indicating possible

mechanisms for selectivity. The most prominent differences were in the central binding site regions (P1, P2 and S1, S2 for  $\text{H}_2\text{PO}_4^-$  and  $\text{SO}_4^{2-}$ , respectively), where relative to  $\text{SO}_4^{2-}$ ,  $\text{H}_2\text{PO}_4^-$  had more contributions from the protein toward the coordinating ligands.

One interesting aspect of the anion-selective channels, particularly  $\text{Cl}^-$  channels, is that selectivity tends to follow the Hofmeister (lyotropic) series; that is, weakly hydrated anions show higher permeability than those binding water molecules more strongly.<sup>36–38</sup> This indicates that the hydration energy is the limiting factor in determining the transport properties of  $\text{Cl}^-$  channels. In our study with the three studied anions, the Hofmeister series can be written as  $\text{SO}_4^{2-} > \text{H}_2\text{PO}_4^- > \text{Cl}^-$ . Sulfate has the strongest hydration and chloride the weakest. With OprP being a wider porin, the transport of smaller anions, for example,  $\text{Cl}^-$ , might not always correspond to the removal of water molecules from the hydration shell, thus making the contribution of the lyotropic sequence toward the selectivity of small ions somewhat less important. However, for larger anions, the selectivity of  $\text{H}_2\text{PO}_4^-$  over  $\text{SO}_4^{2-}$  could well be explained in terms of this effect. It is energetically more costly to remove water molecules from the hydration shell of sulfate than from phosphate.<sup>39</sup> Furthermore, a larger amount of work is required to dehydrate an anion than a cation of similar size.<sup>40</sup> In this context,  $\text{K}^+$  can shed its hydration shell water molecules more easily than  $\text{Cl}^-$ . This is reflected in Figure 4d, where  $\text{K}^+$  stripped more water molecules compared with  $\text{Cl}^-$ , even though the overall electrostatic environment was not favorable for a positively charged ion. This led to a large energetic barrier for  $\text{K}^+$  permeation through the channel (Figure 2).

To this point, we have limited our discussion of ion selectivity of OprP to thermodynamic equilibrium factors, which essentially drive ion-binding selectivity. However these channels are designed to allow the flow of ions. Hence kinetic factors play a role in determining the overall transport processes.<sup>10</sup> In particular, we were interested in analyzing the transitions of  $\text{H}_2\text{PO}_4^-$  or  $\text{SO}_4^{2-}$  ions between the two central binding sites. The role of the residue K121 in the transfer of phosphate from site P1 to P2 has been previously discussed.<sup>23,24</sup> In addition to K121, the role of D94 also needs to be investigated in such transition processes because this aspartate side chain can form hydrogen bonds with the permeating phosphate ion in its monobasic form. The strategically important position of D94 closer to site P2 in OprP (Figure 1c) also provides an opportunity to help phosphate ions to be knocked out of binding site P2 in addition to assisting their transition between the two central binding sites. A similar kind of interaction was not possible in the case of  $\text{SO}_4^{2-}$  due to the absence of any hydrogen bond donor.

As expected, we observed a positive correlation between the  $z$  positions of K121 and  $\text{H}_2\text{PO}_4^-/\text{SO}_4^{2-}$  (Figure 5). It indicated that the dynamics of K121 was coupled to the permeating ions and established its role in transferring these two ions from one central binding site to the other. (See the Supporting Information for details.) A similar analysis with the D94 residue showed a positive correlation for  $\text{H}_2\text{PO}_4^-$  but a lack of any correlation with  $\text{SO}_4^{2-}$  (Figure 5). Correlated movements between D94- $\text{H}_2\text{PO}_4^-$  (one-sample  $t(26) = 2.98$ ,  $p = 0.006$ ), K121- $\text{H}_2\text{PO}_4^-$  (one-sample  $t(26) = 2.26$ ,  $p = 0.032$ ), and K121- $\text{SO}_4^{2-}$  (one-sample  $t(27) = 2.05$ ,  $p = 0.049$ ) were found to be statistically significant while nonsignificant in the case of

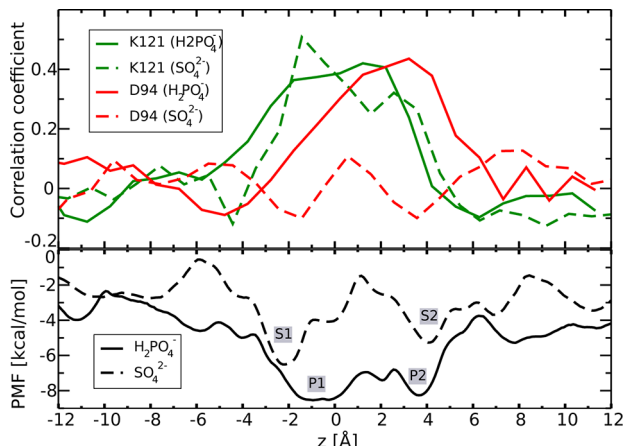


**Figure 5.** Correlated movement of permeating  $\text{H}_2\text{PO}_4^-$  and  $\text{SO}_4^{2-}$  ions with K121 and D94. Respective PMFs for both ions in central binding sites regions are also shown for the sake of comparison.

D94- $\text{SO}_4^{2-}$  (one-sample  $t(27) = 0.80$ ,  $p = 0.428$ ). These findings indicate a possible additional contribution of D94, in conjunction with K121, to transit  $\text{H}_2\text{PO}_4^-$  between two central binding sites. This observation was also reflected in the PMF profiles where  $\text{SO}_4^{2-}$  had an energetic barrier of  $\sim 4$  kcal/mol (from S1 to S2) compared with the smaller energetic barrier of  $\sim 2$  kcal/mol (from P1 to P2) for  $\text{H}_2\text{PO}_4^-$ . Hence the presence or absence of H-bond donors in the permeating ion can influence the energetic costs for ion transfer between the two central binding sites via interactions with D94 and thereby may alter the permeation rates. The functional importance of D94 is also reflected in the evolutionary process as it is conserved among the orthologs of OprP in different *Pseudomonas* species. (See Figure S6 in the Supporting Information.)

In conclusion, we have probed the selectivity of OprP using full atomistic free-energy MD simulation studies. PMF profiles for the permeation of four different ions were obtained. The selectivity of OprP was discussed in the context of well-studied ion channels, especially the  $\text{K}^+$  channel KcsA and anion-selective  $\text{Cl}^-$  channels. The generalized mechanisms of selectivity for OprP can be summarized as a coarse-to-fine scheme in the following order:

1. Although OprP is lined by flexible amino acid side chains ("brush-like" nanopore), the first level of selectivity can be explained based on the "size-exclusion" principle, which is also the case for nonselective porins like OmpF.
2. Discrimination between cations and anions is conferred by the overall electrostatic environment of the channel.
3. The selectivity between ion types of the same charge (cations or anions) results from a fine-tuned balance of interactions between permeating ions and water as well as protein atoms and their corresponding interaction strengths.

In addition, kinetics factors are also important in determining the overall transport properties of ions through a channel. Future studies can be directed toward investigating the role of individual important amino acid residues, for example, those from binding site regions or the arginine ladder, in determining the selectivity and transport properties of OprP. This kind of study might help to delineate detailed structure-function relationship of this porin in particular and broaden our present understanding of ion selectivity of different channels in general.

## ASSOCIATED CONTENT

### S Supporting Information

Details regarding system setup, simulation parameters, and analysis of the results. This material is available free of charge via the Internet at <http://pubs.acs.org/>

## AUTHOR INFORMATION

### Corresponding Author

\*E-mail: u.kleinekathofer@jacobs-university.de.

### Notes

The authors declare no competing financial interest.

## ACKNOWLEDGMENTS

This work has been supported by grants KL 1299/6-1 and BE 865/16-1 of the Deutsche Forschungsgemeinschaft (DFG).

## REFERENCES

- (1) Hille, B. *Ion Channels of Excitable Membranes*, 3rd ed.; Sinauer: Sunderland, MA, 2001.
- (2) Page, M.; Di Cera, E. Role of  $\text{Na}^+$  and  $\text{K}^+$  In Enzyme Function. *Physiol. Rev.* **2006**, 86, 1049–1092.
- (3) Overington, J.; Al-Lazikani, B.; Hopkins, A. How Many Drug Targets Are There? *Nat. Rev. Drug Discovery* **2006**, 5, 993–996.
- (4) Shannon, M.; Bohn, P.; Elimelech, M.; Georgiadis, J.; Marinas, B.; Mayes, A. Science and Technology For Water Purification In the Coming Decades. *Nature* **2008**, 452, 301–310.
- (5) Varma, S.; Rempe, S. Tuning Ion Coordination Architectures To Enable Selective Partitioning. *Biophys. J.* **2007**, 93, 1093–1099.
- (6) Thomas, M.; Jayatilaka, D.; Corry, B. The Predominant Role of Coordination Number In Potassium Channel Selectivity. *Biophys. J.* **2007**, 93, 2635–2643.
- (7) Fowler, P. W.; Tai, K.; Sansom, M. S. The Selectivity of  $\text{K}^+$  Ion Channels: Testing the Hypotheses. *Biophys. J.* **2008**, 95, 5062–5072.
- (8) Shrivastava, I.; Sansom, M. Simulations of Ion Permeation Through a Potassium Channel: Molecular Dynamics of KcsA In a Phospholipid Bilayer. *Biophys. J.* **2000**, 78, 557–570.
- (9) Bernèche, S.; Roux, B. Energetics of Ion Conduction Through the  $\text{K}^+$  Channel. *Nature* **2001**, 414, 73–77.
- (10) Egwulf, B.; Roux, B. Ion Selectivity of the KcsA Channel: A Perspective From Multi-ion Free Energy Landscapes. *J. Mol. Biol.* **2010**, 401, 831–842.
- (11) Noskov, S.; Bernèche, S.; Roux, B. Control of Ion Selectivity in Potassium Channels by Electrostatic and Dynamic Properties of Carbonyl Ligands. *Nature* **2004**, 431, 830–834.
- (12) Cohen, J.; Schulten, K. Mechanism of Anionic Conduction Across CLC. *Biophys. J.* **2004**, 86, 836–845.
- (13) Noskov, S.; Roux, B. Importance of Hydration and Dynamics On the Selectivity of the KcsA and NaK Channels. *J. Gen. Physiol.* **2007**, 129, 135–143.
- (14) Ivanov, I.; Cheng, X.; Steven, M.; McCammon, J. Barriers To Ion Translocation In Cationic and Anionic Receptors From the Cys-loop Family. *J. Am. Chem. Soc.* **2007**, 129, 8217–8224.
- (15) Hajjar, E.; Mahendran, K. R.; Kumar, A.; Bessonov, A.; Petrescu, M.; Weingart, H.; Ruggerone, P.; Winterhalter, M.; Ceccarelli, M. Bridging Timescales and Length Scales: From Macroscopic Flux To the Molecular Mechanism of Antibiotic Diffusion Through Porins. *Biophys. J.* **2010**, 98, 569–575.
- (16) Raj Singh, P.; Ceccarelli, M.; Lovelle, M.; Winterhalter, M.; Mahendran, K. R. Antibiotic Permeation Across the OmpF Channel: Modulation of the Affinity Site In the Presence of Magnesium. *J. Phys. Chem. B* **2012**, 116, 4433–4438.
- (17) Doyle, D.; Cabral, J.; Pfuetzner, R.; Kuo, A.; Gulbis, J.; Cohen, S.; Chait, B.; MacKinnon, R. The Structure of the Potassium Channel: Molecular Basis of  $\text{K}^+$  Conduction and Selectivity. *Science* **1998**, 280, 69–77.
- (18) *Bacterial and Eukaryotic Porins*; Benz, R., Ed.; Wiley-VCH: Weinheim, Germany, 2004.

- (19) Hancock, R. E. W.; Poole, K.; Benz, R. Outer Membrane Protein P of *Pseudomonas Aeruginosa*: Regulation by Phosphate Deficiency and Formation of Small Anion-specific Channels in Lipid Bilayer Membranes. *J. Bacteriol.* **1982**, *150*, 730–738.
- (20) Benz, R.; Egli, C.; Hancock, R. E. W. Anion Transport Through the Phosphate-specific OprP-channel of the *Pseudomonas Aeruginosa* Outer Membrane: Effects of Phosphate, Di-and Tribasic Anions and of Negatively-charged Lipids. *Biochim. Biophys. Acta* **1993**, *1149*, 224–230.
- (21) Benz, R.; Hancock, R. E. W. Mechanism of Ion Transport Through the Anion-Selective Channel of the *Pseudomonas Aeruginosa* Outer Membrane. *J. Gen. Physiol.* **1987**, *89*, 275–295.
- (22) Hancock, R. E. W.; Benz, R. Demonstration and Chemical Modification of a Specific Phosphate Binding Site In the Phosphate-starvation-inducible Outer Membrane Porin Protein P of *Pseudomonas Aeruginosa*. *Biochim. Biophys. Acta* **1986**, *860*, 699–707.
- (23) Moraes, T.; Bains, M.; Hancock, R. E. W.; Strynadka, N. An Arginine Ladder in OprP Mediates Phosphate-specific Transfer Across the Outer Membrane. *Nat. Struct. Mol. Biol.* **2006**, *14*, 85–87.
- (24) Pongprayoon, P.; Beckstein, O.; Wee, C. L.; Sansom, M. S. Simulations of Anion Transport Through OprP Reveal the Molecular Basis For High Affinity and Selectivity For Phosphate. *Proc. Natl. Acad. Sci. U.S.A.* **2009**, *21614*–8.
- (25) Aksimentiev, A.; Schulten, K. Imaging Alpha-hemolysin with Molecular Dynamics: Ionic Conductance, Osmotic Permeability, and the Electrostatic Potential Map. *Biophys. J.* **2005**, *88*, 3745–3751.
- (26) Sotomayor, M.; Vasquez, V.; Perozo, E.; Schulten, K. Ion Conduction Through MscS as Determined by Electrophysiology and Simulation. *Biophys. J.* **2007**, *92*, 886–902.
- (27) Pezeshki, S.; Chimerel, C.; Bessenov, A.; Winterhalter, M.; Kleinekathöfer, U. Understanding Ion Conductance On a Molecular Level: An All-atom Modeling of the Bacterial Porin OmpF. *Biophys. J.* **2009**, *97*, 1898–1906.
- (28) Modi, N.; Singh, P. R.; Mahendran, K. R.; Schulz, R.; Winterhalter, M.; Kleinekathöfer, U. Probing the Transport of Ionic Liquids in Aqueous Solution Through Nanopores. *J. Phys. Chem. Lett.* **2011**, *2*, 2331–2336.
- (29) Biro, I.; Pezeshki, S.; Weingart, H.; Winterhalter, M.; Kleinekathöfer, U. Comparing the Temperature-Dependent Conductance of the Two Structurally Similar *E. coli* Porins OmpC and OmpF. *Biophys. J.* **2010**, *98*, 1830–1839.
- (30) Modi, N.; Winterhalter, M.; Kleinekathöfer, U. Computational Modeling of Ion Transport Through Nanopores. *Nanoscale* **2012**, *4*, 6166–6180.
- (31) Darve, E.; Pohorille, A. Calculating Free Energies Using Average Force. *J. Chem. Phys.* **2001**, *115*, 9169.
- (32) Hénin, J.; Chipot, C. Overcoming Free Energy Barriers Using Unconstrained Molecular Dynamics Simulations. *J. Chem. Phys.* **2004**, *121*, 2904.
- (33) Phillips, J. C.; Braun, R.; Wang, W.; Gumbart, J.; Tajkhorshid, E.; Villa, E.; Chipot, C.; Skeel, R. D.; Kale, L.; Schulten, K. Scalable Molecular Dynamics with NAMD. *J. Comput. Chem.* **2005**, *26*, 1781–1802.
- (34) Allen, T. W.; Andersen, O. S.; Roux, B. Ion Permeation Through a Narrow Channel: Using Gramicidin to Ascertain All-atom Molecular Dynamics Potential of Mean Force Methodology and Biomolecular Force Fields. *Biophys. J.* **2006**, *90*, 3447–3448.
- (35) Chang, C.; Chen, W.; Gilson, M. Ligand Configurational Entropy and Protein Binding. *Proc. Natl. Acad. Sci. U.S.A.* **2007**, *104*, 1534.
- (36) Bormann, J.; Hamill, O.; Sakmann, B. Mechanism of Anion Permeation Through Channels Gated by Glycine and Gamma-aminobutyric Acid In Mouse Cultured Spinal Neurones. *J. Physiol. (London, U. K.)* **1987**, *385*, 243–286.
- (37) Verdon, B.; Winpenny, J.; Whitfield, K.; Argent, B.; Gray, M. Volume-activated Chloride Currents In Pancreatic Duct Cells. *J. Membr. Biol.* **1995**, *147*, 173–183.
- (38) Linsdell, P.; Hanrahan, J. Adenosine Triphosphate-dependent Asymmetry of Anion Permeation In the Cystic Fibrosis Transmembrane Conductance Regulator Chloride Channel. *J. Gen. Physiol.* **1998**, *111*, 601–614.
- (39) Zhang, J.; Kamenev, A.; Shklovskii, B. I. Ion Exchange Phase Transitions In Water-filled Channels with Charged Walls. *Phys. Rev. E* **2006**, *73*, 051205.
- (40) Hummer, G.; Pratt, L.; Garca, A. Free Energy of Ionic Hydration. *J. Phys. Chem.* **1996**, *100*, 1206–1215.